A tale of winglets: evolution of flight morphology in stick insects

Supplementary Materials

Text section

Notes on ancestral state reconstruction for relative wing size in stick insects

Figures

S1, Summary of morphological sampling
S2, Summary of wing diversity in Necrosciini
S3, Bayesian species tree inferred with BEAST
S4, Summary of phylogenetic correlations for flight morphology among winged stick insects
S5, Ancestral state reconstruction for relative wing size
S6, Ancestral state reconstruction for body size
S7, Ancestral state reconstruction for sexual size dimorphism (SSD) and sexual wing dimorphism (SWD)

Tables

S1, Information on nuclear and mitochondrial loci
S2, Summary of PGLS results for all winged stick insects
S3, Summary of derived wing functions for stick insects with miniaturized wings

Datasets

1. Morphometrics (taxon, wing length, body length)
2. Scaling of wing loading (body mass, wing length, wing area)
3. Molecular sampling (list of species), including accession numbers for new sequences on GenBank
4. Nexus input files
5. Alignment files
6. BEAST input file

Script

MatLab script for organizing taxonomic data from Phasmida Species Files

Supplementary Text

Notes on ancestral state reconstruction for wing size evolution in stick insects

Our maximum-likelihood ancestral state reconstruction showed that a short relative wing size ($Q < 0.4$) preceded multiple gains and losses observed in extant phasmids (**Fig. S5**). Nevertheless, this result offered only a preliminary perspective on wing size evolution in phasmids, as it reflects but a small portion of extant phasmid diversity (~ 10% documented species). A complete molecular phylogeny and comprehensive trait sampling are not currently available.

Preliminary sampling for the presence of hindwings showed a highly variable pattern across phasmid clades, even below the subfamily level (**Fig. S1, S2**). Note the use of Linnean ranks (tribes) here only serves for a preliminary categorization of wing size variation before phylogenies with higher resolution become available (also, see Zachos, 2011; Lambertz and Perry, 2016). Given the non-monophyletic status of some tribes (e.g., Xeroderini and Eurycanthini) and the large variation of age between main lineages (e.g., see **Fig. S3**), we expect a more complex wing evolution pattern in future phylogenetic analyses.

In order to properly model evolutionary rates of change and to reconstruct ancestral states for relative wing size, future work should increase phylogenetic resolution and incorporate trait sampling across extant tips. Properly modeling gain and loss of wings in phasmids will require complex models to account for (1) variation in the rate of wing size evolution across the tree (Beaulieu et al. 2013), and (2) variation in rates of species diversification across the tree (Maddison 2006). In particular, Goldberg and Igić (2008) suggested that the loss and gain of wings may affect diversification patterns. Our results demonstrating a bimodal distribution of wing size further indicated a more complex and wing size-dependent diversification scenario.

Supplementary Figures

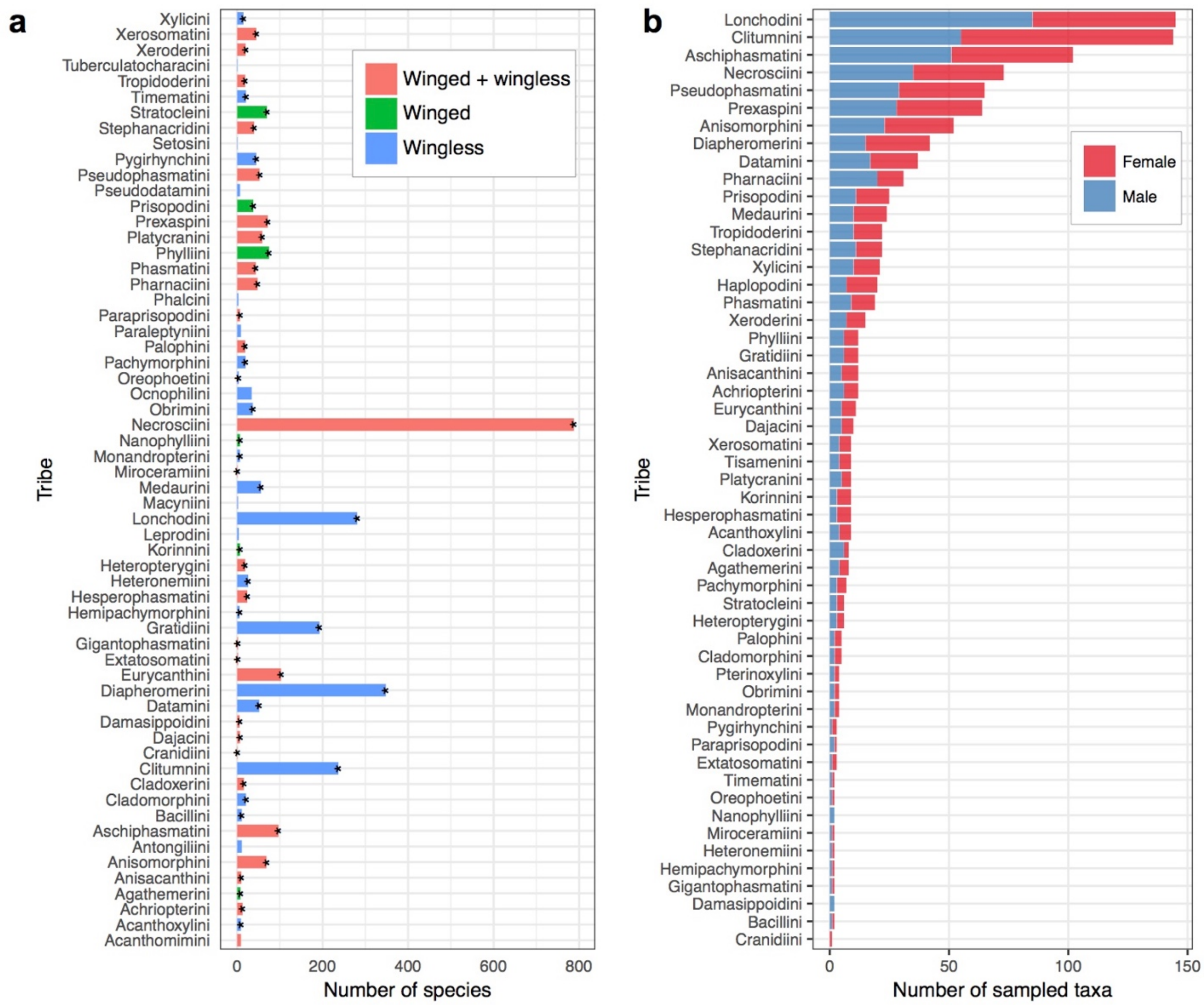

Figure S1. Summary of taxa sampled for flight-related morphology in this study. (a) All documented phasmid tribes, with the number of species based on Brock et al. (2019). Colors represent the hindwing condition within tribes; asterisks denote tribes sampled in this study. (b) Summary of the number of taxa sampled for hindwing size (see **Supplementary Dataset 1**). Note the use of tribes here is only to convenient a preliminary categorization of wing size variation without a detailed phylogeny.

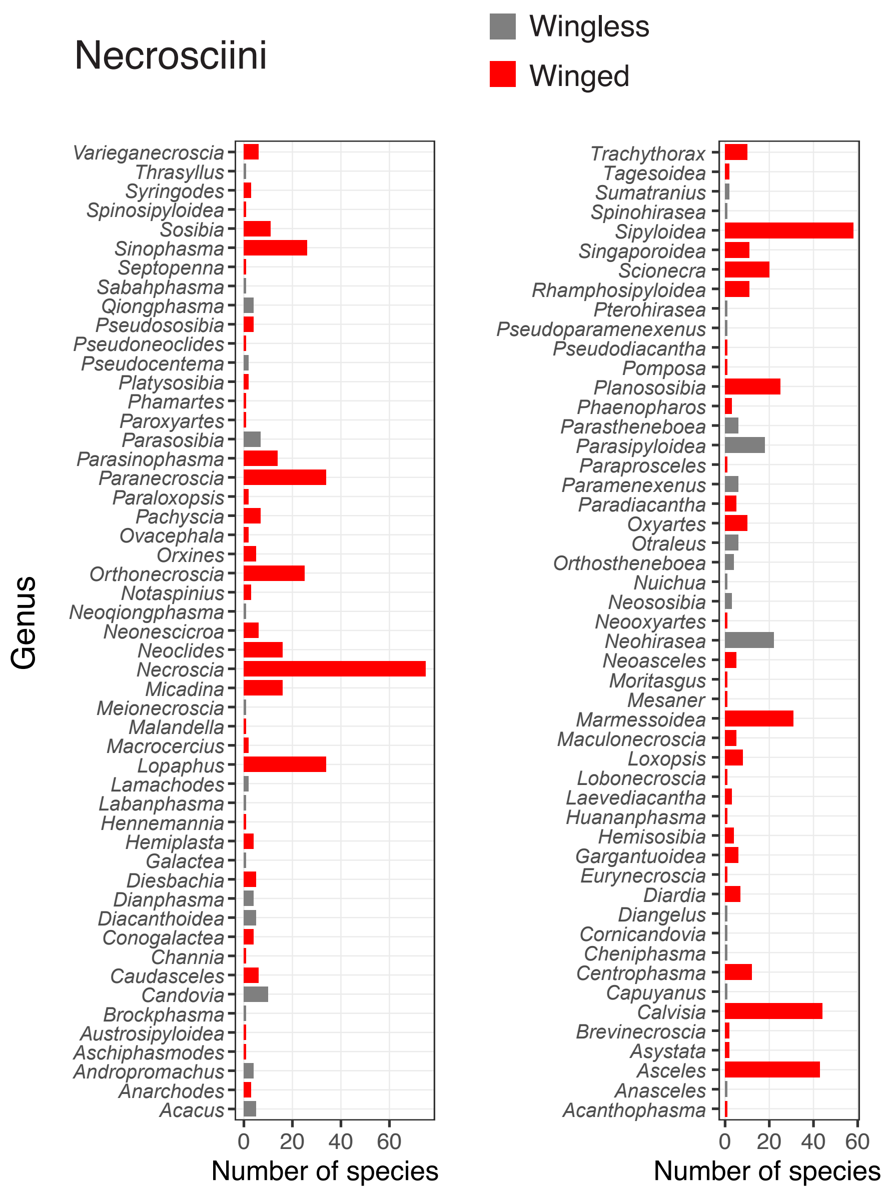

Figure S2. A summary for the presence of hindwings and the number of species among genera of the tribe Necrosciini. Taxonomic organization followed Phasmida Species File (Brock, 2019). This demonstrates the high variability of wing morphology, which is greatly underexplored, even at a lower level.

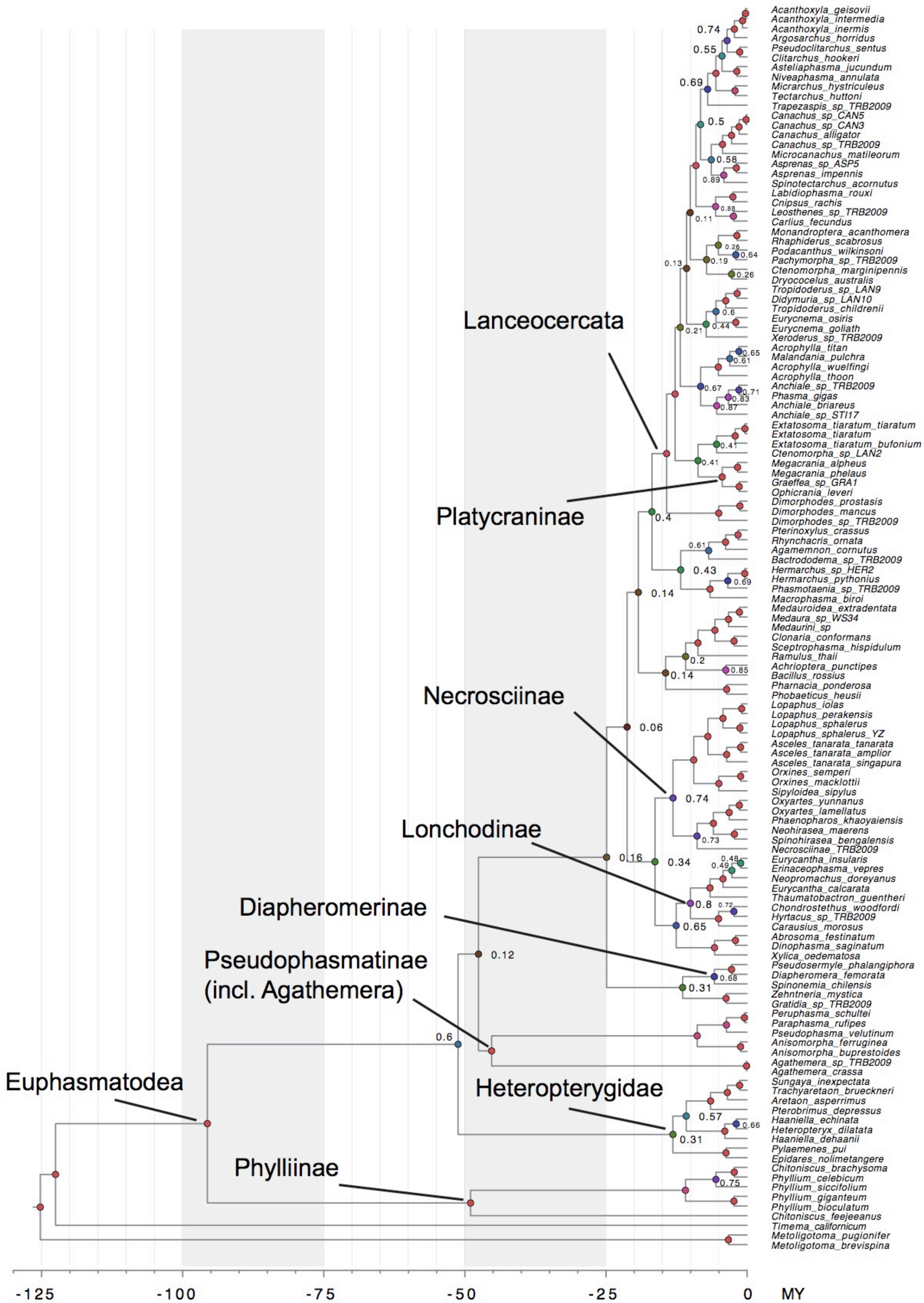

Figure S3. Bayesian species tree inferred with BEAST, with node labels showing posterior probabilities < 0.9 and node color representing the posterior.

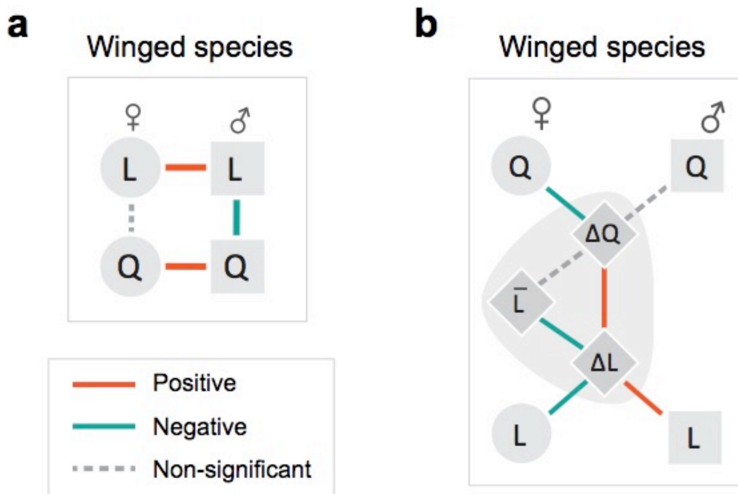

Figure S4. Phylogenetic correlations between wing and body size among winged species. Details are provided in **Table S2**.

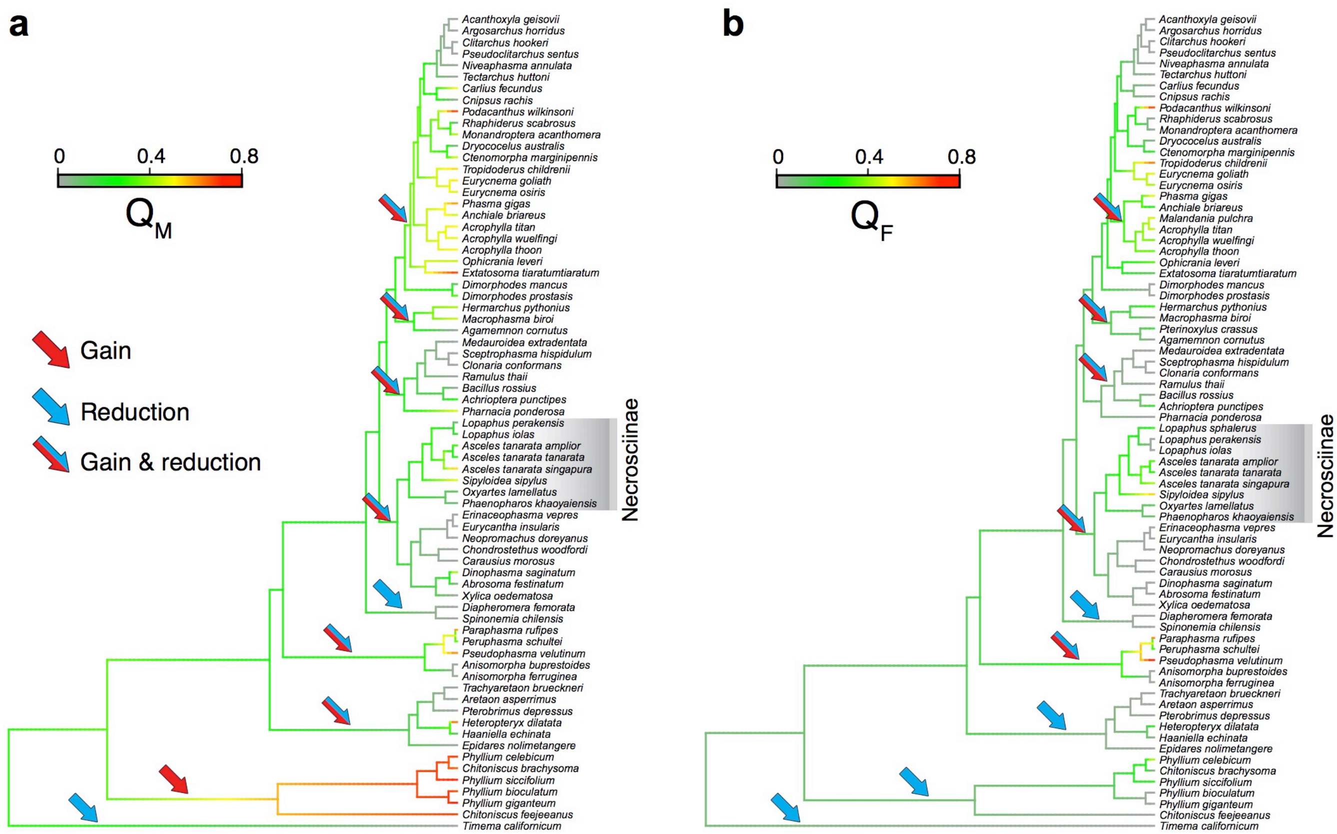

Figure S5. Ancestral state reconstruction for relative wing size (Q) of males (a) and females (b), respectively, featuring repeated gain and reduction. The last common ancestor of the main clades is characterized by short wings ($Q < 0.4$); however, this inference is liable to change with more complete sampling. Arrows on main branches highlight increases and reductions of wing size. In long-wing lineages (e.g., Necrosciinae), relative wing size between females and males is correlated (see **Fig. 7a**).

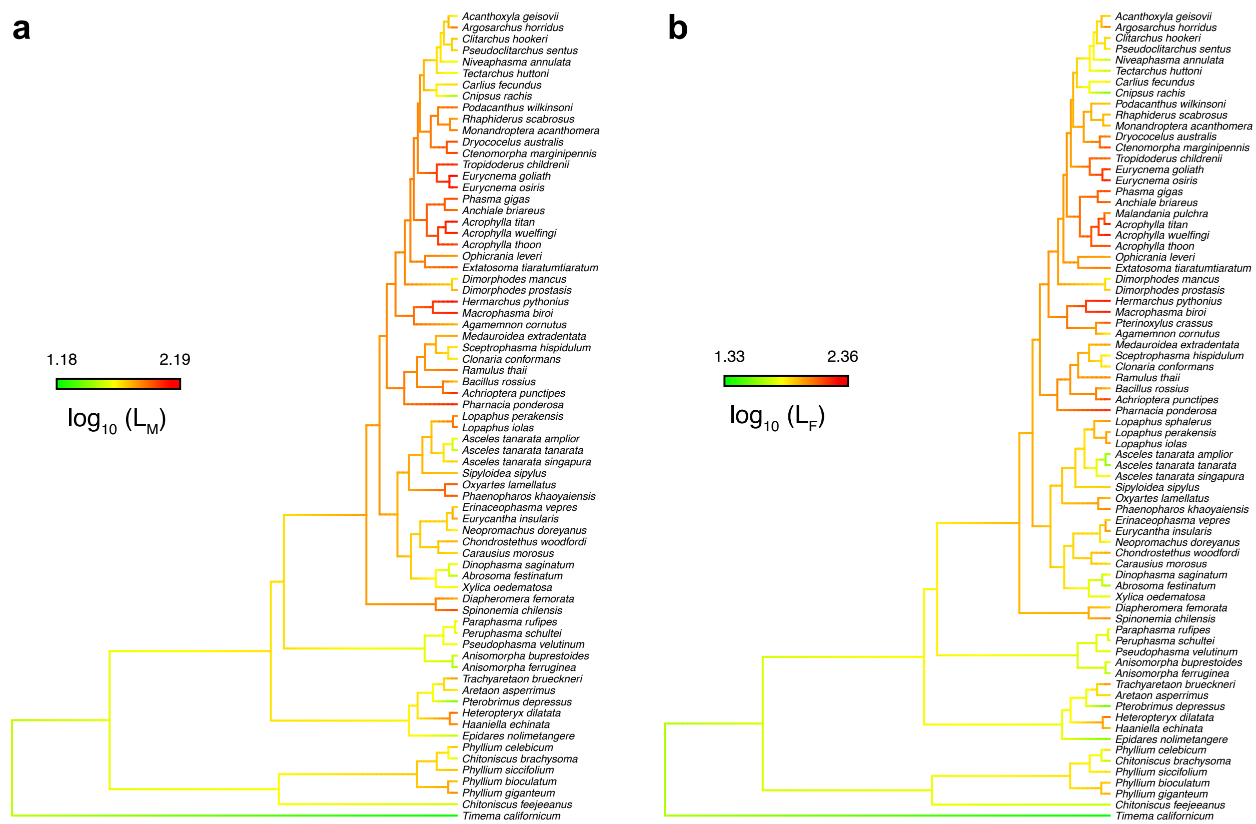

Figure S6. Ancestral state reconstruction for body size (L) of males (a) and females (b), respectively. Body size evolution is coupled between two sexes but independent of wing size evolution, corresponding with the correlational pattern summarized in **Fig. 7a**.

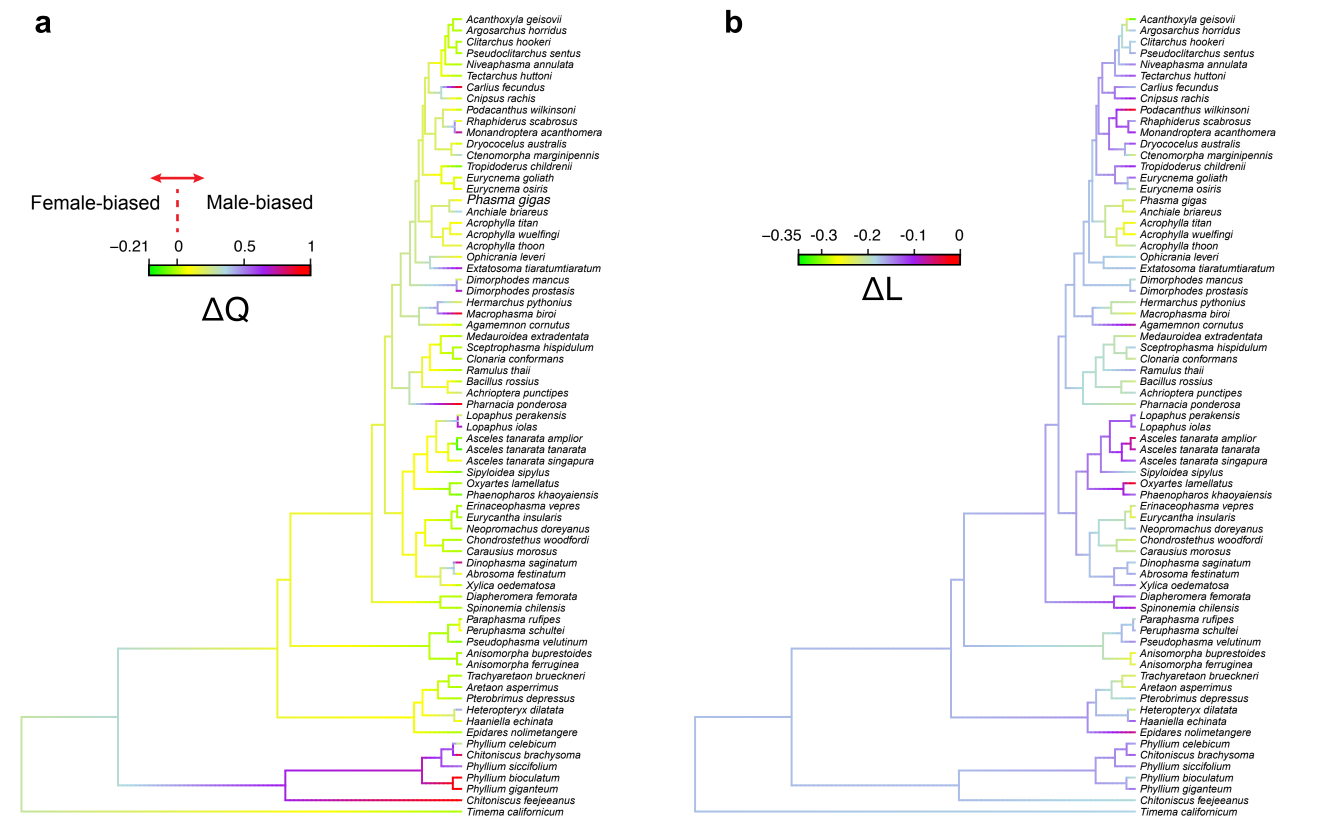

Figure S7. Ancestral state reconstruction for sexual wing dimorphism (SWD) index (ΔQ; a) and sexual size dimorphism (SSD) index (ΔL; b). (a) The ancestral state reconstruction of ΔQ shows repeated increases and reductions, with an intermediate level of male-biased SWD ($0 < \Delta Q < 0.5$, as represented by yellow color) as the ancestral state for most clades. (b) Ancestral state reconstruction of ΔL, showing an intermediate level of female-biased SSD ($-0.2 < \Delta L < -0.1$) as the ancestral state preceding repeated increase and reduction. The lack of evolutionary correlation between ΔL and ΔQ, as summarized in **Fig. 7c**, is evident by comparing (a) and (b).

Supplementary Tables

Locus	Forward primer	Reverse primer	T_a (˚C)	Length (bp)	Reference
28s	AGAACTTTGAAGAGAGAGTTCAAGA	TCAAGACGGGTCGGGAGA	50	495	Buckley et al., 2009
COI	TTGATTTTTTGGTCATCCAGAAGT	TCCAATGCACTAATCTGCCATATTA	50	814	Simon et al., 1994
COII	AATATGCAGATTAGTGCA	GTTTAAGAGACCAGTACTTG	50	736	Simon et al., 1994
H3	ATGGCTCGTACCAAGCAGAC	ATATCCTTRGGCATRATRGTGAC	50	358	Buckley et al., 2009

Table S1. Information on the nuclear and mitochondrial loci used in this study.

		PGLS			
	correlations	***N***	**slope**	**slope.SE**	***P***
Male	Q_M ~ $Log_{10}(L_M)$ ‡	273	-0.271 (0.005)	0.072 (0.001)	< 0.001
Female	Q_F ~ $Log_{10}(L_F)$ ‡	262	-0.107 (0.02)	0.1 (0.001)	0.296 (0.096)
Wing size, species-wise comparison	Q_F ~ Q_M ‡	158	0.876 (0.01)	0.063 (0.001)	< 0.001
	Q_M ~ ΔQ	183	-0.029 (0.003)	0.038 (0)	0.438 (0.04)
	Q_F ~ ΔQ ‡	158	-0.534 (0.007)	0.068 (0)	< 0.001
	ΔQ ~ ΔL ‡	158	-0.637 (0.033)	0.22 (0.003)	0.005 (0.003)
	ΔQ ~ L_{mean} ‡	158	0.001 (0)	0.001	0.332 (0.11)
Body size, species-wise comparison	L_M ~ L_F	367	0.61 (0.001)	0.014 (0)	< 0.001
	L_F ~ ΔL	367	-118.893 (5.122)	18.92 (0.38)	< 0.001
	L_M ~ ΔL	367	31.48 (3.534)	13.999 (0.276)	0.03 (0.02)
	ΔL ~ L_{mean}	158	0	0	0.03 (0.026)

Table S2. Summary of pairwise correlational analyses applied to all winged species using PGLS models. Values represent means from analyses using 100 randomly resolved trees, with 1 s.d. in brackets. The symbol ‡ indicates that equivalent significance was found for analyses using the original data with variables converted to pseudo-continuous ordinal numbers in analyses (see Methods).

Taxa	Stridulation	Startle display	Reference
Pterinoxylus spinulosus female and male	x	x	Robinson, 1968
Hanniella spp. female and male	x		Pers. Observ.
Oxyartes spp. female and male		x	Pers. Observ.
Phaenopharus spp. female and male		x	Pers. Observ.
Diapherodes spp. female		x	Pers. Observ.
Parectatosoma spp. female and male		x	Pers. Observ.
Diesbachia hellotis female		x	Pers. Observ.
Achrioptera spp. female and male		x	Pers. Observ.
Peruphasma spp. female and male		x	Pers. Observ.

Table S3. A summary of known cases of derived wing utility in stick insects with miniaturized wings.

References

Beaulieu, J. M., O'Meara, B. C. and Donoghue, M. J. (2013). Identifying hidden rate changes in the evolution of a binary morphological character: the evolution of plant habit in campanulid angiosperms. *Syst Biol* **62**, 725-737.

Brock, P., Büscher, T. and Baker, E. (2019). *Phasmida Species File Online Version 5.0.*

Buckley, T. R., Attanayake, D. and Bradler, S. (2009). Extreme convergence in stick insect evolution: phylogenetic placement of the Lord Howe Island tree lobster. *Proceedings of the Royal Society B: Biological Sciences* **276**, 1055-1062.

Goldberg, E. E. and Igić, B. (2008). On phylogenetic tests of irreversible evolution. *Evolution* **62**, 2727-2741.

Lambertz, M. and Perry, S. F. (2016). Again on the meaning of categorial ranks in modern evolutionary biology? *Organisms Diversity & Evolution* **16**, 723-725.

Maddison, W. P. (2006). Confounding asymmetries in evolutionary diversification and character change. *Evolution* **60**, 1743-1746.

Simon, C., Frati, F., Beckenbach, A., Crespi, B., Liu, H. and Flook, P. (1994). Evolution, weighting, and phylogenetic utility of mitochondrial gene sequences and a compilation of conserved polymerase chain reaction primers. *Annals of the entomological Society of America* **87**, 651-701.

Zachos, F. E. (2011). Linnean ranks, temporal banding, and time-clipping: why not slaughter the sacred cow? *Biological Journal of the Linnean Society* **103**, 732-734.